Facile in situ Formation of CuO/ZnO p-n Heterojunction for Improved H$_2$S-sensing Applications

Arunkumar Shanmugasundaram[1†], Dong-Su Kim[1†], Tian Feng Hou[1†], and Dong Weon Lee[1,2+]

Abstract

In this study, hierarchical mesoporous CuO spheres, ZnO flowers, and heterojunction CuO/ZnO nanostructures were fabricated via a facile hydrothermal method. The as-prepared materials were characterized in detail using various analytical methods such as powder X-ray diffraction, micro Raman spectroscopy, X-ray photoelectron spectroscopy, field-emission scanning electron microscopy, and transmission electron microscopy. The obtained results are consistent with each other. The H$_2$S-sensing characteristics of the sensors fabricated based on the CuO spheres, ZnO flowers, and CuO/ZnO heterojunction were investigated at different temperatures and gas concentrations. The sensor based on ZnO flowers showed a maximum response of ~141 at 225 °C. The sensor based on CuO spheres exhibited a maximum response of 218 at 175 °C, whereas the sensor based on the CuO/ZnO nano-heterostructure composite showed a maximum response of 344 at 150 °C. The detection limit (DL) of the sensor based on the CuO/ZnO heterojunction was ~120 ppb at 150 °C. The CuO/ZnO sensor showed the maximum response to H$_2$S compared with other interfering gases such as ethanol, methanol, and CO, indicating its high selectivity.

Keywords: H$_2$S sensor, p-CuO, n-ZnO, p-n heterojunction, high sensitivity, selectivity

1. INTRODUCTION

Air pollutants emitted by industries and automobiles cause several health problems and raise various environmental concerns. Among various air pollutants, hydrogen sulfide (H$_2$S) is a colorless, highly toxic, and flammable gas classified as a chemical asphyxiant [1]. According to the Occupational Safety and Health Administration of the USA, the threshold limit value of H$_2$S is 10 ppm for 8 h, and the short-term exposure limit value is 15 ppm for 15 min [1]. H$_2$S instantly reacts with hemoglobin in blood and damages the human body by blocking the cellular respiration and nervous systems [1,2]. Early noninvasive diagnosis of several lung diseases can be performed by measuring and monitoring the

H$_2$S concentration in exhaled human breath [3]. Therefore, developing a highly efficient H$_2$S sensor is required for assuring human and environmental safety.

Over the years, several gas-sensing techniques have been developed for the detection of toxic and flammable gases [4,5]. Among them, nanostructured metal-oxide-based gas sensors are considered promising devices owing to their large surface area, high sensitivity, a wide range of detection limits, facile construction, low power consumption, low cost, fast response and recovery times, and compatibility with microelectronic fabrication processing. To date, several metal-oxide-based gas sensors such as NiO [1,2], SnO$_2$ [6], CuO [7], ZnO [8], and In$_2$O$_3$ [9-11] have been developed for the detection and quantification of H$_2$S. Among several metal oxides, CuO has received significant attention owing to its excellent physical and chemical properties [7]. To date, several CuO-based nanostructure sensors have been studied extensively for H$_2$S-sensing applications. For instance, Li et al. developed a room-temperature high-performance H$_2$S sensor based on porous CuO nanosheets. The sensor showed an excellent response of 1.25 to 10 ppb of H$_2$S at ambient temperature [7]. Sonia et al. prepared a CuO-thin-film-based H$_2$S sensor, which exhibited a response of ~34% with the response and recovery times of 107 and 127 s toward 2 ppm of H$_2$S, respectively, at 200 °C [12]. Although the proposed sensors showed excellent responses to H$_2$S gas, the response and recovery times of the

[†] These authors contributed equally to this work: Arunkumar Shanmugasundaram, Dong-Su Kim, Tian Feng Hou
[1] Graduate School of Mechanical Engineering, Chonnam National University, 77, Yongbong-ro, Buk-gu, Gwangju, 61186, Korea
[2] Center for Next Generation Sensor Research and Development, Chonnam National University, 77, Yongbong-ro, Buk-gu, Gwangju, 61186, Korea
[+] Corresponding author: mems@jnu.ac.kr

sensor were very high, and the sensors were operated at very high temperatures (<250 °C).

Recently, several strategies have been developed to improve the H_2S-gas-sensing performance of metal-oxide-based gas sensors. One such strategy is the incorporation of metal nanoparticles such as Au, Pt, Pd, and Ag [6]. For instance, Rai et al. developed Au@NiO yolk-shell nanostructures, which showed a high response of 108.92 toward 5 ppm of H_2S [13]. However, using metal nanoparticles is not advantageous from an economic perspective owing to their higher price [10]. Another strategy is the incorporation of doped reduced-graphene-oxide (RGO) into the metal-oxide matrix. For example, Shanmugasundaram et al. developed nitrogen-boron co-doped RGO-incorporated NiO nanodisks for improved H_2S-sensing applications [1]. Other strategies include light illumination, which activates the adsorption sites for the gas molecules, and a combination of materials forming a p-n heterojunction. As an example of the latter strategy, Sun et al. demonstrated an improved H_2S-sensing performance of Fe_2O_3-nanoparticle-decorated NiO nanoplate sensors [14].

In continuation of these efforts, we present a CuO/ZnO p-n-type nano-heterostructure sensor for an improved H_2S-sensing application. The CuO/ZnO p-n-type nano-heterostructure was prepared via a facile hydrothermal method using copper nitrate trihydrate and zinc nitrate hexahydrate as metal precursors, ethanolamine as an organic Lewis base, and water as the reaction medium. The H_2S-sensing characteristics of the sensors fabricated based on ZnO flowers, CuO spheres, and CuO/ZnO heterostructure were investigated at different operating temperatures (30 °C < Ts < 250 °C) and gas concentrations (5 ppm < Gc < 500 ppm). Gas-sensing studies revealed that the CuO/ZnO p-n heterostructure composite shows improved H_2S-sensing characteristics over pristine CuO and ZnO nanostructures. The selectivity of the sensor was investigated in the presence of other interfering gases such as ethanol, methanol, carbon monoxide, and nitrogen dioxide.

2. EXPERIMENTAL

2.1 Material

Copper nitrate trihydrate ($Cu(NO_3)_2.3H_2O$), zinc nitrate hexahydrate ($Zn(NO_3)_2.6H_2O$), and ethanolamine ($NH_2CH_2CH_2OH$) were purchased from Sigma-Aldrich. All the chemicals were analytical reagent (AR) grade and used without further

purification. Deionized water (18.2 MΩ at 25 °C) was used throughout the experiment.

2.2 Preparation of ZnO nanoflowers

According to a typical synthesis process, 1 mmol of zinc nitrate hexahydrate was dissolved in 30 mL of deionized water under constant magnetic stirring, and subsequently, 6 mmol of ethanolamine was added. After 30 min of stirring, the solution was transferred to a Teflon-lined autoclave, heated to 150 °C in a programmable oven, and maintained at that temperature for 12 h. Subsequently, the autoclave was oven-cooled to room temperature. The product was separated using a centrifugation process, purified by washing with deionized water and ethanol, and then dried at 100 °C for 12 h.

2.3 Preparation of CuO hierarchical nanospheres

According to a typical synthesis process, 4 mmol of copper nitrate trihydrate was dissolved in 30 mL of deionized water under uniform magnetic stirring, and subsequently, 6 mmol of ethanolamine was added. After 30 min of stirring, the solution was transferred to the Teflon-lined autoclave, heated to 150 °C in a programmable oven, and maintained at that temperature for 12 h. Subsequently, the autoclave was oven-cooled to room temperature. The product was separated using a centrifugation process, purified by washing with deionized water and ethanol, and then dried at 100 °C for 12 h.

3. RESULTS AND DISCUSSIONS

The morphologies of the as-prepared materials were characterized using field-emission scanning electron microscopy (FESEM) and transmission electron microscopy (TEM). Fig. 1 shows the FESEM images of the as-synthesized hierarchical mesoporous CuO spheres at different magnifications. The low-magnification FESEM image shows nearly monodispersed CuO spheres along with some broken parts of the spheres (Fig. 1a). The high-resolution image demonstrates the high surface roughness of the as-prepared material (Fig. 1b). Further, the high-magnification image shows the hierarchical mesoporous nature of the obtained material (Fig. 1c). Each of these CuO spheres is composed of several nanorods of size ~50 nm. Fig. 1d shows the top-view of the as-prepared CuO spheres, indicating the formation of hexagonal nanorods. The FESEM analysis demonstrates that the
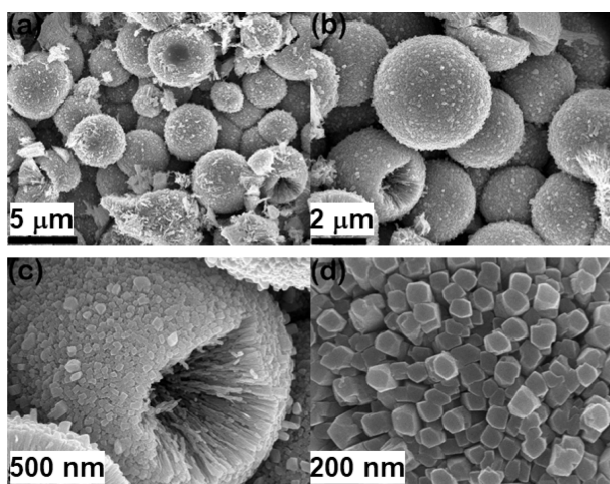
Fig. 1. (a-d) FESEM images of the as-prepared hierarchical mesoporous CuO spheres at different magnifications
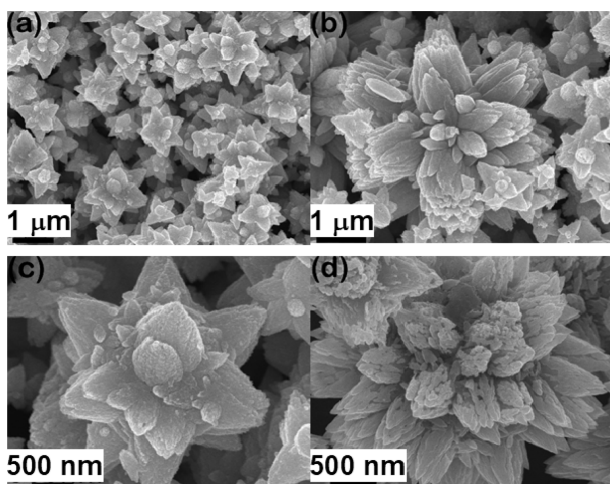

Fig. 3. (a-d) FESEM images of the as-prepared hierarchical mesoporous CuO/ZnO nano-heterostructures at different magnifications

Fig. 2. (a-d) FESEM images of the as-prepared hierarchical mesoporous ZnO flowers at different magnifications

Fig. 4. (a-b) TEM images of the as-prepared hierarchical mesoporous CuO/ZnO nano-heterostructures at different magnifications; (c) the high-resolution TEM image of the CuO/ZnO nano-heterostructure; and (d) selected-area electron diffraction image of the CuO/ZnO nano-heterostructure

CuO spheres are secondary structures, and are the building blocks of the primary nanorod structures.

The low-magnification FESEM image shows the numerous as-prepared ZnO flowers with a uniform shape and a size of ~2 μm (Fig. 2a). The high-magnification FESEM image shows the hierarchical nature of the as-prepared ZnO flowers. Each of these flowers is assembled by secondary spindles of size ~500 nm, which radiate from the center core of the material. (Fig. 2 b,c). Interestingly, each spindle is the assembly of several nanoparticles with an average diameter of ~20 nm (Fig. 2d). Fig. 3 shows the FESEM images of the as-prepared CuO/ZnO heterostructure at different magnifications. The low-magnification FESEM shows several CuO spheres along with numerous ZnO flowers (Fig. 3a). The high-magnification FESEM image demonstrates that the ZnO
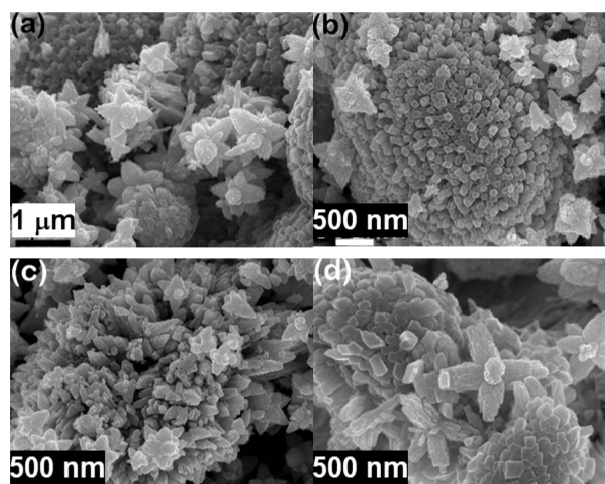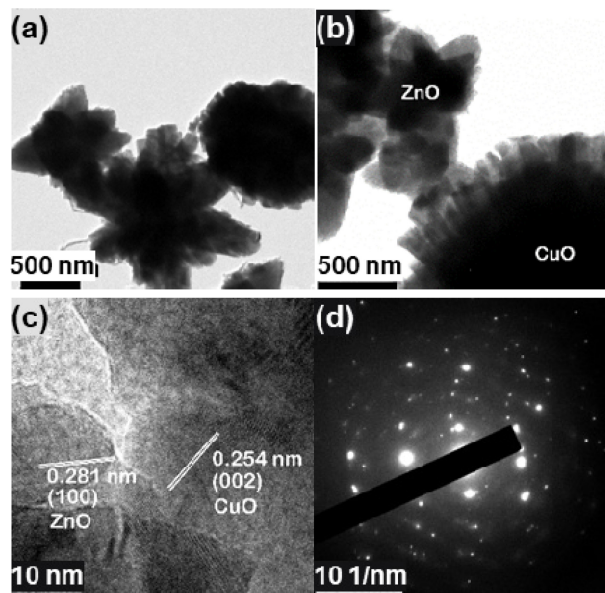
flowers are anchored on the CuO spheres, indicating the formation of in situ p-n nano-heterostructures.

Fig. 4 shows the TEM images of the as-prepared CuO/ZnO nano-heterostructure at different magnifications. The low-magnification image shows the presence of well-defined CuO spheres and ZnO flowers. The high-magnification image demonstrates the hierarchical nature of the as-prepared materials. The electron-dense and impoverished region indicates the
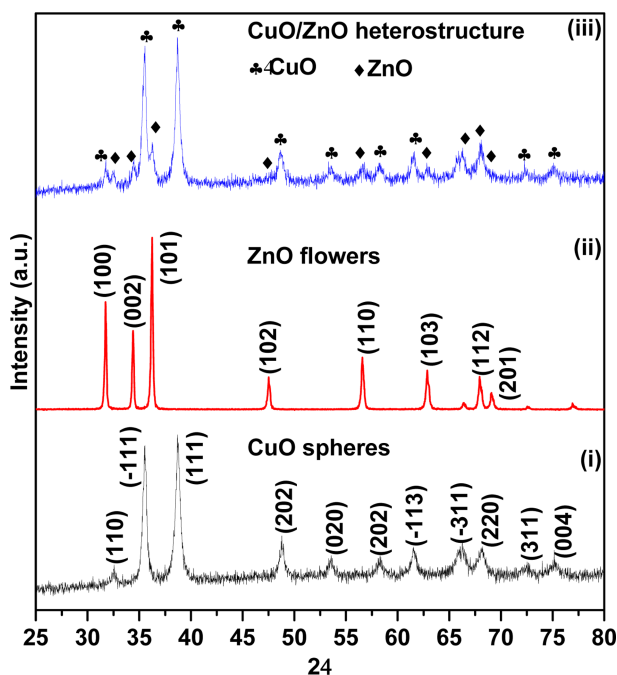
Fig. 5. Powder XRD pattern of the as-prepared (i) CuO spheres, (ii) ZnO flowers, and (iii) hierarchical mesoporous CuO/ZnO nano-heterostructure

Fig. 6. X-ray photoelectron spectra of the as-prepared CuO/ZnO heterostructure composite. (a) Survey spectra and core-level spectra; the high-resolution core-level spectra of (b) Cu2p; (c) Zn2p; and (d) O1s

mesoporous nature of the as-prepared materials. The high-resolution TEM image shows an interplanar spacing of ~0.281 nm corresponding to the (100) plane of the wurtzite ZnO crystal structure [15]. The other interplanar spacing of ~0.281 nm can be attributed to the (002) plane of the cubic CuO crystal structure [16]. The Laue spots in the selected-area electron diffraction pattern indicate the polycrystalline nature of ZnO and CuO.

The crystal structure, phase purity, and formation of the composite of the as-prepared materials were characterized using powder X-ray diffraction (XRD). Fig. 5(i) shows the XRD pattern of the as-prepared CuO spheres. All the diffraction patterns can be indexed to the cubic CuO crystal structure. The sharp and strong diffraction pattern of CuO indicates the highly crystalline nature of the as-prepared material. The diffraction peaks in Fig. 5(ii) at the 2θ values of 31.80°, 34.41°, 36.21°, 47.52°, 56.53°, 62.74°, 67.80°, and 69.11° can be assigned to the (100), (002), (101), (102), (110), (103), (112), and (201) planes, respectively, of the wurtzite ZnO crystal structure with the space group of P63 mc (186) [15]. Fig. 5(iii) shows the XRD pattern of the as-prepared CuO/ZnO nano-heterostructure, which confirms the successful formation of the CuO/ZnO composite. No other crystalline phase corresponding to any impurity was detected, indicating the high purity of the synthesized product.

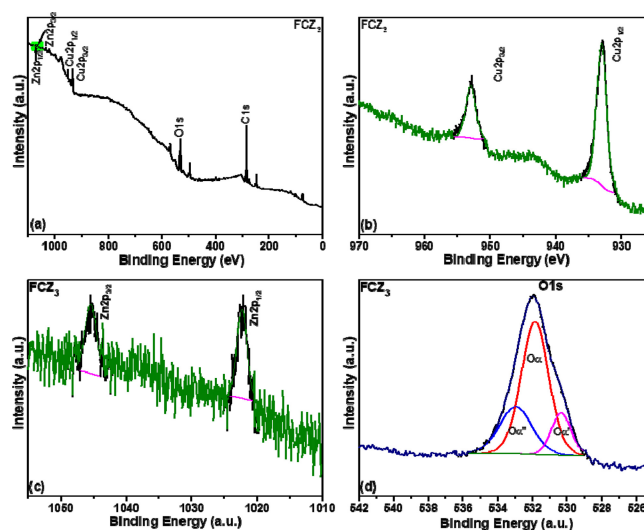Further, the as-prepared CuO/ZnO nano-heterostructure

composite was characterized using X-ray photoelectron spectroscopy. The survey spectra show the photoelectron peaks of Zn, Cu, and O (Fig. 6a). No other photoelectron peaks were observed, indicating the pure phase formation of the CuO/ZnO composite. Fig. 6 (b, c) shows the high-resolution core-level spectra of the as-prepared CuO/ZnO composite in the copper and zinc regions. The peaks observed at 952.6 and 934.6 eV can be assigned to the spin-orbit splitting of Cu $2p_{3/2}$ and Cu $2p_{1/2}$, respectively [17, 18]. The peaks observed at 1022.71 and 1045.52 eV correspond to Zn $2p_{3/2}$ and Zn $2p_{1/2}$, respectively [8]. Fig. 6d shows the high-resolution core-level spectra of the as-prepared CuO/ZnO composite in the oxygen region. The peaks at 531.2 eV are attributed to the lattice oxygen, whereas the peaks at 532.2 and 533.5 eV can be indexed to the chemisorbed oxygen and adsorbed molecular oxygen, respectively [8].

The gas-sensing characteristics of the sensors fabricated based on the CuO spheres, ZnO flowers, and CuO/ZnO nano-heterostructure composites were investigated as a function of the operating temperature (30 °C < Ts < 250 °C) toward 50 ppm of H₂S. As shown in Fig. 7a, the sensor response increased with increasing operating temperature. The sensor based on ZnO flowers showed the maximum response of ~141 at 225 °C, and its response decreased with a further increase in the temperature. The sensor based on CuO spheres exhibited a maximum response of 218 at 175 °C, whereas the sensor based on the CuO/ZnO nano-heterostructure composite showed a maximum response of 344 at 150 °C.

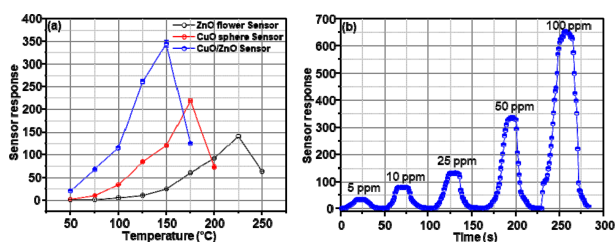Arunkumar Shanmugasundaram, Dong-Su Kim, Tian Feng Hou, and Dong Weon Lee

Fig. 7. (a) Sensing response characteristics of the sensors based on the CuO spheres, ZnO flowers, and CuO/ZnO heterostructure composite as a function of different operating temperatures toward 50 ppm of H_2S. (b) Dynamic sensing response representing the response and recovery times of the fabricated CuO/ZnO heterostructure composite sensor at 150 °C as a function of different H_2S gas concentrations.

Fig. 8. Response and recovery times of the CuO/ZnO heterostructure composite sensor toward 50 ppm of H_2S at an operating temperature of 150 °C. Selectivity of the CuO/ZnO heterostructure composite sensor toward 10 ppm of ethanol, methanol, CO, hexane, and H_2S at 150 °C.

Further, the sensing response of the CuO/ZnO composite sensor was investigated at 150 °C toward different concentrations of H_2S (5 ppm < Gc < 500 ppm). As shown in Fig. 7b, the sensor response gradually increased at higher H_2S concentrations. The responses of the CuO/ZnO composite sensor at 150 °C were 43, 88, 142, 345, and 662 toward 5, 10, 25, 50, and 100 ppm of H_2S, respectively. The dynamic sensing characteristics demonstrate a wide range of detection limits. The DL of the CuO/ZnO heterostructure composite sensor at 150 °C was calculated using the following equation (1) [19, 20]. The DL of the sensor was ~120 ppb at 150 °C.

$$S = 3 \times \frac{RMSnoise}{Slope} \qquad (1)$$

The response and recovery times of the sensor were investigated at 150 °C toward 50 ppm of H_2S (Fig. 8a). The response and recovery times of the sensor were 27 and 12 s, respectively. The selectivity of the CuO/ZnO composite sensor was investigated in the presence of other interfering gases. Fig. 8b shows the response of the CuO/ZnO composite sensor to 10 ppm of ethanol, methanol, CO, hexane, and H_2S at 150 °C. The sensor showed the maximum response of ~72 to H_2S, whereas its responses to ethanol, methanol, and CO were ~12, 14, and 9, respectively, indicating its highly selective nature.

The highest sensitivity of the CuO/ZnO composite sensor can be explained by considering the following significant factors. The first factor is the hierarchical mesoporous nature of the as-prepared material. The as-prepared material is composed of several ultrafine nanostructures that remarkably improve the depletion regions of the sensing element. Such conditions are desirable for an ultrahigh sensing response [11]. Second, the high surface area and mesoporosity of the CuO/ZnO composite provide
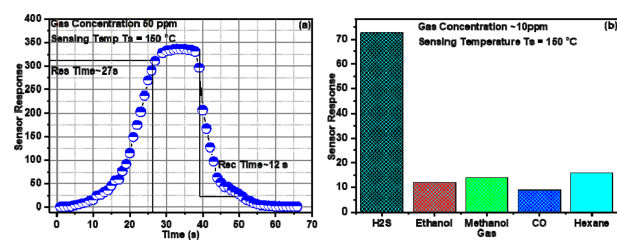
abundant active surface area for gas adsorption and offer numerous pathways for the diffusion of the gas molecules, thereby enhancing the gas kinetics reaction [10]. Finally, the heterojunctions formed between the CuO and ZnO interfaces facilitate an enhanced transport of free electrons from ZnO into CuO across the junction because of the downward shift of the Fermi level in the ZnO grains. The heterojunction between n-ZnO/p-CuO produced a band bending across the interface between n-ZnO/p-CuO, which increased the mobility (μ) of the charge carriers and hence improved the sensor response [6, 20-22].

4. CONCLUSIONS

In summary, CuO spheres, ZnO flowers, and CuO/ZnO heterostructures were successfully synthesized via a facile hydrothermal method. The as-prepared materials were characterized in detail using different analytical techniques, and the obtained data were consistent with each other. The gas-sensing characteristics of the fabricated sensors were investigated at different operating temperatures and gas concentrations. The gas-sensing studies revealed that the formation of the CuO/ZnO heterostructure led to a dramatic improvement in H_2S-sensing performance. The sensor based on the CuO/ZnO heterostructure composite showed a maximum response of 344 at 150 °C, whereas the pristine ZnO flower and CuO sphere sensors exhibited the maximum responses of ~141 at 225 °C and 218 at 175 °C, respectively. The enhanced sensing response of the CuO/ZnO heterostructure sensor is attributed to the synergetic effect between CuO and ZnO.

ACKNOWLEDGMENT

REFERENCES

[1] A. Shanmugasundaram, N. D. Chinh, Y.-J. Jeong, T. F. Hou, D.-S. Kim, D. Kim, Y. B. Kim, and D.-W. Lee, "Hierarchical nanohybrids of B- and N-codoped graphene/mesoporous NiO nanodisks: an exciting new material for selective sensing of H₂S at near ambient temperature", *J. Mater. Chem. A*, Vol. 7, 9263-9278, 2019.

[2] S. K. Ganapathi, M. Kaur, R. Singh, V. Singh, A. K. Debnath, K. P. Muthe, and S. C. Gadkari. "Anomalous Sensing Response of NiO Nanoparticulate Films towards H₂S", *ACS App. Nano Mater.*, Vol. 2, No. 10, pp. 6726-6737, 2019.

[3] D. Zhang, Z. Wu, and X. Zong, "Flexible and highly sensitive H₂S gas sensor based on in-situ polymerized SnO₂/rGO/PANI ternary nanocomposite with application in halitosis diagnosis". *Sens. Actuator B*, Vol. 289, No. 15, pp. 32-41, 2019.

[4] G. K. Naik, and Y. T. Yu, "Synthesis of Au@TiO₂ Core-shell Nanoparticle-decorated rGO Nanocomposite and its NO₂ Sensing Properties", *J. Sens. Sci. Technol.*, Vol. 28 No. 4, pp. 225-230, 2019.

[5] S. Y. Yi, Y. G. Song, G. S. Kim, and C.-Y. Kang, "In-decorated NiO Nanoigloos Gas Sensor with Morphological Evolution for Ethanol Sensors", *J. Sens. Sci. Technol.*, Vol. 28 No. 4, pp. 231-235, 2019.

[6] A. Shanmugasundaram, P. Basak, L. Satyanarayana, and S. V. Manorama, "Hierarchical SnO/SnO₂ nanocomposites: Formation of in situ p–n junctions and enhanced H₂ sensing", *Sens. Actuators B*, Vol. 185, No. pp. 265-273, 2013.

[7] Z. Li,, N. Wang, Z. Lin, J. Wang, W. Liu, K. Sun, Y. Q. Fu, and Z. Wang, "Room-Temperature High-Performance H₂S Sensor Based on Porous CuO Nanosheets Prepared by Hydrothermal Method", *ACS App. Mater. Interfaces*, Vol. 8 No. 32, pp. 20962-20968, 2016.

[8] S. Arunkumar, T. Hou, Y. B. Kim, B. Choi, S. H. Park, S. Jung and D. W. Lee, "Au Decorated ZnO Hierarchical Architectures: Facile Synthesis, Tunable Morphology and Enhanced CO Detection at Room Temperature", *Sens. Actuators B*, Vol. 243, pp. 990-1001, 2017.

[9] A. Shanmugasundaram, B. Ramireddy, P. Basak, S. V. Manorama, and S. Srinath, "Hierarchical In(OH)₃ as a Precursor to Mesoporous In₂O₃ Nanocubes: A Facile Synthesis Route, Mechanism of Self-Assembly, and Enhanced Sensing Response toward Hydrogen", *J. Phys. Chem. C*, Vol. 118, No. 13. pp. 6909-6921, 2014.

[10] A. Shanmugasundaram, V. Gundimeda, T. F. Hou, and D. W. Lee, "Realizing synergy between In₂O₃ nanocubes and nitrogen-doped reduced graphene Oxide: An excellent nanocomposite for the selective and sensitive detection of CO at ambient temperatures", *ACS Appl. Mater. Interfaces*, Vol. 9, No. 37, pp. 31728-31740, 2017.

[11] A. Shanmugasundaram, P. Basak, S. V. Manorama , B. Krishna, and S. Srinath,, "Hierarchical Mesoporous In₂O₃ with Enhanced CO Sensing and Photocatalytic Performance: Distinct Morphologies of In(OH)₃ via Self Assembly Coupled in Situ Solid–Solid Transformation", *ACS App. Mater. Interfaces*, Vol. 7, No. 14, pp. 7679-7689, 2015.

[12] S. Sonia, P. Sureshkumar, N. D. Jayram, Y. Masuda, D. Mangalaraj, and C. Lee, "Superhydrophobic and H₂S gas sensing properties of CuO nanostructured thin films through a successive ionic layered adsorption reaction process", *RSC Adv.,* Vol. 6, pp. 24290-24298, 2016.

[13] P. Rai, J. W. Yoon, H. M. Jeong, S. J. Hwang, C. H. Kwak, and J. H. Lee, Design of Highly Sensitive and Selective Au@NiO Yolk-Shell Nanoreactors for Gas Sensor Applications, *Nanoscale*, Vol. 6, pp. 8292-8299, 2014.

[14] G. J. Sun, H. Kheel, J. K. Lee, S. Choi, S. Lee, and C. Lee, "H₂S gas sensing properties of Fe₂O₃ nanoparticle-decorated NiO nanoplate sensors", *Surf. Coat. Technol.*, Vol. 307, pp. 1088-1095, 2016.

[15] A. Shanmugasundaram, R. Boppella, Y. J. Jeong, J. Park, Y. B. Kim, B. Choi, S. H. Park, S. Jung, and D. W. Lee, "Facile In-Situ Formation of RGO/ZnO Nanocomposite: Photocatalytic Remediation of Organic Pollutants under Solar Illumination", *Mater. Chem. Phys.*, Vol. 218, pp. 218-228, 2018.

[16] Y. Zhai, Y. Ji, G. Wang, Y. Zhu, H. Liu, Z. Zhong, and F. Su, "Controllable wet synthesis of multicomponent copper-based catalysts for Rochow reaction", *RSC Adv.*, Vol. 5, pp. 73011-73019, 2015.

[17] S. Masudy-Panah, R.S. Moakhar, C. S. Chua, H. R. Tan, T. I. Wong, D. Chi, and G. K. Dalapati, "Nanocrystal Engineering of Sputter-Grown CuO Photocathode for Visible-Light-Driven Electrochemical Water Splitting", *ACS Appl. Mater. Interfaces*, Vol. 8, No. 2, pp. 1206-1213, 2016.

[18] Q. Li, Q. Wei, L. Xie, C. Chen, C. Lu, F. Y. Su, and P. Zhou, "Layered NiO/Reduced Graphene Oxide Composites by Heterogeneous Assembly with Enhanced Performance as High-Performance Asymmetric Supercapacitor Cathode", *RSC Adv.*, Vol. 6, pp. 46548-46557, 2016.

[19] Z. Song, Z. Wei, B. Wang, Z. Luo, S. Xu, W. Zhang, H. Yu, M. Li, Z. Huang, J. Zang, F. Yi, and H. Liu, "Sensitive Room-Temperature H₂S Gas Sensors Employing SnO2 Quantum Wire/Reduced Graphene Oxide Nanocomposites", *Chem. Mater.*, Vol. 28, pp. 1205-1212, 2016.

[20] C. V. G. Reddy, and S.V. Manorama, "Room Temperature Hydrogen Sensor Based on SnO2:La2O3", *J. Electrochem. Soc.*, Vol. 147, pp. 390-393, 2000.

[21] S. Arunkumar, P. Basak, L. Satyanarayana, and S. Manorama, "One-pot Hydrothermal Synthesis of SnO and SnO₂ Nanostructures: Enhanced H2 Sensing Attributed to in-situ p-n Junctions", *14th Int. Meet. on Chem. Sens.,* pp. 372-375, Nuremberg, Germany, 2012.

[22] R. Boppella, P. Manjula, S. Arunkumar, and S. V Manorama, "Advances in synthesis of nanostructured metal oxides for chemical sensors", *Chem. Sens.*, Vol. 4, pp. 19(1)-19(20), 2014.